NTNU Trondheim
Norwegian University of Science and Technology
Department of Marine Technology

TMR4240 Marine Control Systems - Project 1

By:

Abubakar Aliyu BADAWI

Ishfaq Ahmad BHAT

Celil YILMAZ

Tayyab TAHIR

Specialization: Marine and Maritime Intelligent Robotics [MIR]

Submitted to:

Prof. Dong Trong Nguyen

Contents

1 Introduction **1**

2 Theory **2**

2.1 Reference Frame . . . 2

2.2 Process Plant Model . . . 2

2.2.1 Vessel Dynamics . . . 3

2.2.2 Wave-frequency Process Plant Model . . . 4

2.2.3 Kinematics . . . 4

2.3 Control Plant Model . . . 5

2.3.1 Low-frequency Control Plant Model . . . 6

2.3.2 Wave-frequency Control Plant Model . . . 7

2.3.3 Bias Model . . . 7

2.3.4 Measurements . . . 8

3 Environmental Loads **8**

3.1 Current Model . . . 8

3.1.1 Surface currents . . . 8

3.1.2 Simulink Implementation of the Current Model . . . 9

3.2 Wind Model . . . 10

3.3 Mean Wind Component . . . 10

3.4 Slowly Varying Component . . . 11

3.5 Simulink Implementation of the Wind Model . . . 11

4 Reference Model **12**

4.1 Implementation of the Reference Model . . . 13

4.2 Tuning of the Reference Model . . . 14

5 Trust Allocation **14**

5.1 Thrusters . . . 15

5.2 Linear Effector Model . . . 15

5.3 Simulink Implementation of the Thrust Allocations . . . 17

6 Controller Design **18**

6.1 Proportional-Integral-Derivative (PID) Control . . . 18

6.2 Implimentation of the PID Controller . . . 19

6.3 Tunning of the PID 20

7 Simulation Results **20**

7.1 Simulation 1 20

7.1.1 Simulation 1A - Current set to 0.5[m/s] from east. 21

7.1.2 Discussion 21

7.1.3 Simulation 1B - Wind with average speed of 10[m/s] from south. 22

7.1.4 Discussion 22

7.2 Simulation 2 23

7.2.1 Simulation 2 - current vary linearly from 0.5[m/s] coming from North to 0.5 [m/s] coming from East, while keeping the vessel at the origin [0 0 0]. 24

7.2.2 Discussion 24

7.3 Simulation 3 25

7.3.1 Vessel Dynamics Without Reference Model 25

7.3.2 Vessel Dynamics With Reference Model 26

7.3.3 Discussion 27

7.4 Reference Model Velocity Trajectories 27

7.4.1 Discussion 28

7.5 Simulation 4 28

7.5.1 4 Corner Test Results 29

7.5.2 Discussion 29

7.5.3 Reference Model Velocity Trajectories 30

7.5.4 Discussion 30

List of Figures

1 Vessel Model 1

2 Reference frame 3

3 Low-frequency (LF) and wave-frequency (WF) motion 3

4 6 DOF Motion for Marine Vessels 5

5 Current Simulink Model 9

6 WInd Relative Angle Calculation 10

7 Wind direction variation around mean value 11

8 Wind Simulink Model 12

9 Umean with Noise 12

10 Simulink Reference Model 13
11 Thrust Allocation Block 17
12 PID Controller Block 19
13 Simulation 1a Results 21
14 SImulation 1b Results 22
15 Change of *North* and *East* current components over time as the current direction varies from 180° to 270° over a 200-second period. 23
16 Simulation 2 Results 24
17 Simulation 3 Results (Without reference model) 26
18 Simulation 3 Results (With reference model) 26
19 Simulation 3 Velocity Trajectories 28
20 Simulation 4 Results 29
21 4 Coner Test Velocity Trajectories 30

List of Tables

1 Final tuning parameters for the reference model 14
2 Thruster positions and angles. 15
3 Final PID controller gains 20

1 Introduction

This project is developed using the MSS Toolbox (Marine Systems Simulator), a MATLAB/Simulink library designed for simulating marine systems. MSS includes models for various marine vessels, such as ships, underwater vehicles, and floating structures. Additionally, it provides guidance, navigation, and control (GNC) blocks for real-time simulations.

The objective of this project is to design a controller, a reference model, and an external load system for the dynamic positioning of a ship. The controller will be tuned to ensure that the system follows the reference model behavior. For this purpose, a PID controller will be implemented.

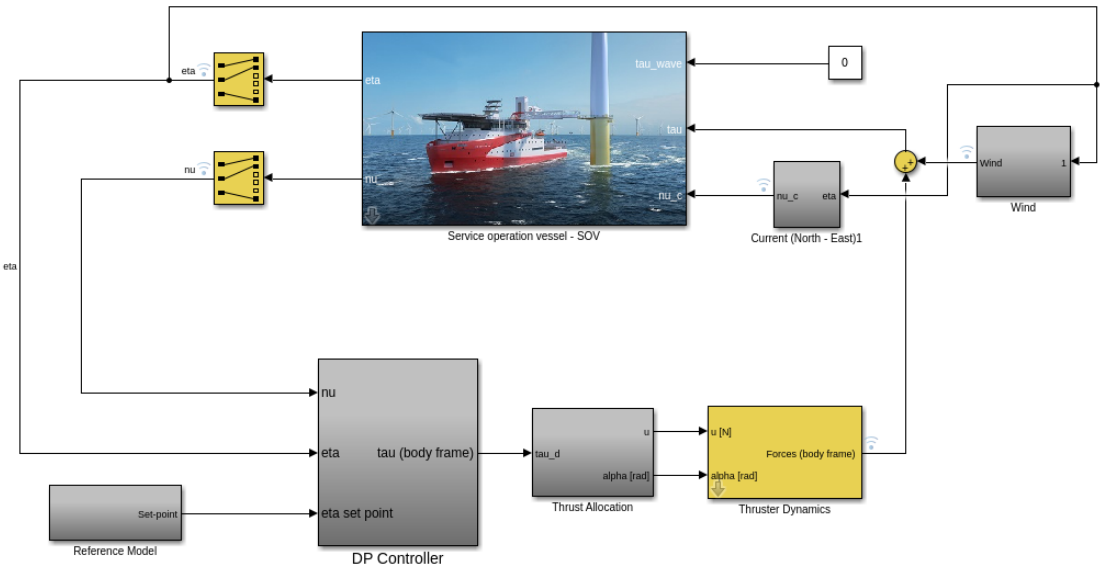

Figure 1: Vessel Model

The vessel's mathematical model, including the equations of motion and the hydrodynamic coefficients utilized in simulations, was prepared in SIMULINK. This report introduces a reference frame employed throughout these simulations. It includes discussions on theories pertinent to process plant modeling and control plant modeling. A mathematical model for the vessel's control plant is proposed, aimed at assisting the design of a potential observer. The reference model used in the simulations is detailed herein. A suitable controller has been selected and implemented for optimizing DP functionality through tuning.

Several tests are necessary to demonstrate the functionality and reliability of the developed systems. These tests are described in the subsequent sections and cover various scenarios that are typical in DP-positioning tasks. Each scenario helps to validate different capabilities of the dynamic positioning system under various conditions and set-point changes.

The document presents a sequence of four simulations to evaluate the dynamic positioning (DP) system under diverse conditions:

1. **Simulation 1:** Tests the DP system's response to environmental forces with a steady current from the east and varying wind from the south. The objective is to maintain a set-point of $\begin{bmatrix} 0 & 0 & 0 \end{bmatrix}$ and observe the system's stability in xy-plots and individual position and heading

plots until steady state is achieved.

2. **Simulation 2:** Examines the system's performance when the current direction changes linearly, initially from the east, without wind interference. The simulation extends until steady state to ensure the system adjusts and maintains the correct heading and position, depicted in xy and individual plots.

3. **Simulation 3:** Compares vessel position over time from a static starting point to a dynamic setpoint, both with and without a reference model. The scenario excludes environmental forces to isolate control system performance, with results displayed in trajectory and velocity plots.

4. **Simulation 4:** Conducts a DP 4-corner test, challenging the system to accurately navigate and stabilize at sequential setpoints without environmental effects. This critical test confirms the system's precision in transitioning and holding positions and headings as planned.

These simulations collectively verify the DP system's capability to perform under varying operational conditions, ensuring its readiness for real-world maritime tasks. Each test is designed not only to validate the functionality and accuracy of the DP system but also to simulate potential real-life scenarios that the vessel might encounter. The successful completion of these simulations will significantly contribute to the confidence in deploying the system for operational duties on supply vessels, particularly in challenging maritime environments where precision and reliability are paramount.

2 Theory

2.1 Reference Frame

As a reference frame for the vessels motions, the North-East-Down- (NED), and body-fixed frame were used. The NED-frame is a tangent plane to the earth's surface and is denoted as:

$$\{n\} = [x_n, y_n, z_n]^T \tag{1}$$

where x_n follows true north, y_n follows east and z_n is positive pointing downwards.

The body-fixed frame corresponds to the vessels different directions and is denoted as:

$$\{b\} = [x_b, y_b, z_b]^T \tag{2}$$

where x_b corresponds to the vessels longitudinal direction, y_b corresponds to transverse directions and z_b points in a direction normal to x_b and y_b.

The Earth-centered Earth-fixed (ECEF) frame (x_e, y_e, z_e) is rotating with an angular rate ω_e with respect to an Earth-centered inertial (ECI) frame (x_i, y_i, z_i) fixed in space.

2.2 Process Plant Model

The process plant model, or simulation model, is a mathematical model of the physical process. In the case of a supply vessel there is a desire to simulate the real world dynamics. The process plant

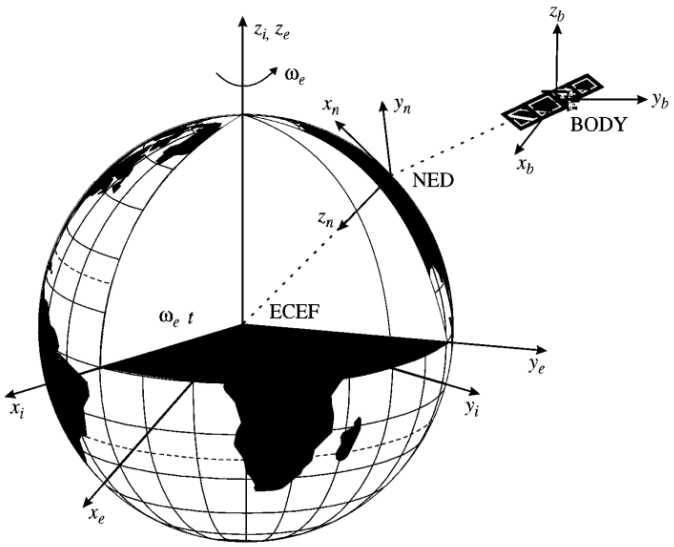

Figure 2: Reference frame
Taken from: handbook of marine craft hydrodynamics and motion control

model gives the necessary detailed descriptions of the vessels dynamics as well as external forces and moments from thrusters and environmental loads.

2.2.1 Vessel Dynamics

When modeling vessel dynamics, it is common to separate the total model into two components using superposition. The first is a wave-frequency model and the second is a low-frequency model, which is referred to as the wave frequency (WF) and low frequency (LF) model respectively. Thus, the total motion becomes a sum of the WF and LF models.

The WF-motions are caused by first order wave loads, while the LF-motions are assumed to be the result of second-order mean and slowly varying wave loads, current loads, wind loads, and thrust forces.

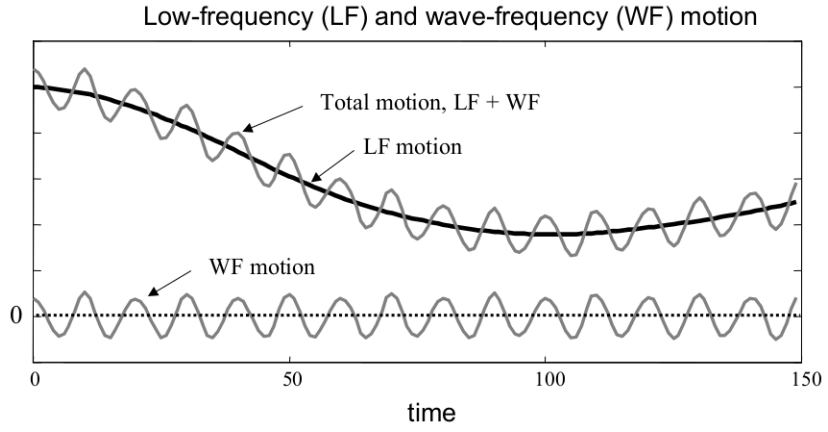

Figure 3: Low-frequency (LF) and wave-frequency (WF) motion
Taken from: handbook of marine craft hydrodynamics and motion control

2.2.2 Wave-frequency Process Plant Model

The behavior of first order linear waves is solved as two separate sub-problems, wave reaction and wave excitation. Which is respectively forces due to the vessel being forced to oscillate with the waves and forces due to the vessel being restrained from oscillation. The lecture notes (Sørensen [2018]) express the solution to the respective problems by:

$$M(\omega)\ddot{\eta}_{Rw} + D_p(\omega)\dot{\eta}_{Rw} + G\eta_{Rw} = \tau_{wave1} \tag{3}$$

$$\eta_w = J(\eta_2)\dot{\eta}_{Rw} \tag{4}$$

Where $\eta_2 = [0, 0, \psi_d]^T$

2.2.3 Kinematics

The study of the dynamics of a vessel can be divided into kinematics and kinetics. Kinematics focuses on the geometrical aspects of motion, while kinetics deals with the analysis of forces that cause motion. This section defines the motion variables, reference frames, and the transformations between these frames (Fossen, 2011, Chapter 2).

DOF		Forces and moments	Linear and angular velocities	Positions and Euler angles
1	motions in the x direction (surge)	X	u	x
2	motions in the y direction (sway)	Y	v	y
3	motions in the z direction (heave)	Z	w	z
4	rotation about the x axis (roll, heel)	K	p	ϕ
5	rotation about the y axis (pitch, trim)	M	q	θ
6	rotation about the z axis (yaw)	N	r	ψ

For marine craft moving in six degrees of freedom (DOF), six independent coordinates are required to determine the position and orientation. The first three coordinates and their time derivatives correspond to position and translational motion along the x, y, and z axes. The last three coordinates, along with their time derivatives, describe the orientation and rotational movement (Fossen T.I., page 15) [3]. These variables lead to the SNAME notation for marine vessels, as shown in Table 1. The vectors η, representing position and Euler angles, and ν, representing linear and angular velocities, are used to describe the motion.

When analyzing the motion of marine craft in 6 DOF, it is useful to define two Earth-centered coordinate frames, along with several geographic reference frames. Fossen defines the Earth-centered frames as the "Earth-Centered Inertial" (ECI) frame and the "Earth-Centered, Earth-Fixed" (ECEF) frame.

The following coordinate frames are commonly used in marine navigation and control:

- **ECI** $i = (x_i, y_i, z_i)$: An inertial frame used for terrestrial navigation. It is non-accelerating and follows Newton's laws of motion, with its origin at the center of the Earth.
- **ECEF** $e = (x_e, y_e, z_e)$: This frame has its origin at the Earth's center but rotates relative to the ECI frame. It is typically used for global navigation and control, such as intercontinental travel.

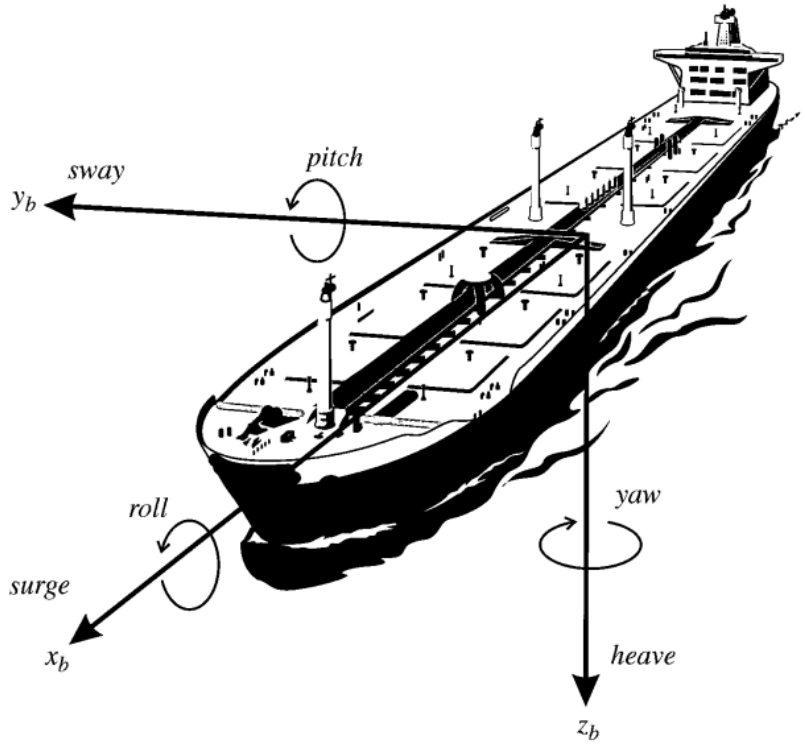

Figure 4: 6 DOF Motion for Marine Vessels
Taken from: handbook of marine craft hydrodynamics and motion control

- **NED** $n = (x_n, y_n, z_n)$: A local coordinate system often defined as a tangent plane at the Earth's surface. The x and y axes point towards true North and East, while the z axis points downwards. The position of n relative to e is determined by the latitude (l) and longitude (μ).
- **BODY** $b = (x_b, y_b, z_b)$: A coordinate frame fixed to the vessel, moving with it. The x_b axis represents the longitudinal axis (aft to fore), y_b the transverse axis (to starboard), and z_b the normal axis (top to bottom). This frame is typically used to express the vessel's linear and angular velocities.

2.3 Control Plant Model

Compared to the process plant model in Section 3, the purpose of a control plant model is to capture the essential behavior of the system, i.e., the most necessary physical characteristics of the model, and not the details. These models are formulated based on careful model reduction or simplification, resulting in a low-fidelity model. The control plant model can constitute a part of the controller and can be used for analytical stability analysis.

In this project, the control plant model is divided into four sub-problems: low-frequency (LF), high-frequency (or wave-frequency, WF), bias, and measurements. While part 1 only considered the low-frequency components, part 2 expands to include all four sub-models.

The system of equations representing the control plant model is given by:

$$\dot{\zeta} = \mathbf{A}_w \zeta + \mathbf{E}_w \mathbf{w}_w \tag{5}$$

$$\dot{\eta} = \mathbf{R}(\psi)\nu \tag{6}$$

$$\dot{\mathbf{b}} = -\mathbf{T}_b^{-1}\mathbf{b} + \mathbf{E}_b \mathbf{w}_b \tag{7}$$

$$\dot{\nu} = -\mathbf{M}^{-1}\mathbf{D}\nu + \mathbf{M}^{-1}\mathbf{R}^T(\psi)\mathbf{b} + \tau \tag{8}$$

$$\mathbf{y} = \eta + \eta_w + \mathbf{w} \tag{9}$$

The variables and matrices used in these equations are described in the following subsections:

- **Equation (5)** describes the wave-frequency dynamics with ζ as the state variable, $\mathbf{A}_w$ as the system matrix, and $\mathbf{E}_w\mathbf{w}_w$ representing the wave input disturbance.
- **Equation (6)** represents the kinematic equation, where η is the position and orientation vector, $\mathbf{R}(\psi)$ is the rotation matrix as a function of the yaw angle ψ, and ν is the velocity vector.
- **Equation (7)** models the dynamics of the bias, where $\mathbf{b}$ is the bias vector, $\mathbf{T}_b^{-1}$ is the inverse time constant matrix, and $\mathbf{E}_b\mathbf{w}_b$ represents the input disturbance for the bias.
- **Equation (8)** describes the low-frequency velocity dynamics, where $\mathbf{M}$ is the mass matrix, $\mathbf{D}$ is the damping matrix, and τ represents external forces acting on the system.
- **Equation (9)** defines the measurement equation, where $\mathbf{y}$ is the measured output, including the true position η, wave-induced motion η_w, and a measurement noise term $\mathbf{w}$.

This is a linear model based on assumptions of small waves and motion amplitudes. By including wave excitation and reaction forces, one can solve the hydrodynamic problem of the vessel. This approach assumes potential theory and neglects viscous effects.

2.3.1 Low-frequency Control Plant Model

Low-frequency (LF) motions are assumed to be caused by second-order mean, slowly-varying loads from wind, current, waves, and forces from the mooring and thrust.

In the low-frequency model, Equation (4) is reduced from 6 DOF to 3 DOF of interest: surge, sway, and yaw (all in the horizontal plane). This simplification is appropriate due to the large vessel size, which results in self-stabilizing behavior in vertical motion. Therefore, it is more convenient for controller design and analysis to derive this nonlinear LF control plant model.

By simplifying Equation (4), we obtain the following reduced equations for the LF model:

$$\dot{\eta} = \mathbf{R}(\psi)\nu \tag{10}$$

$$\mathbf{M}\dot{\nu} + \mathbf{D}\nu + \mathbf{R}^T(\psi)\mathbf{G}(\eta) = \tau + \mathbf{R}^T(\psi)\mathbf{b} \tag{11}$$

where $\nu = [u, v, r]^T$, $\eta = [x, y, \psi]^T$, and $\mathbf{b} \in R^3$ is the bias vector. Additionally, $\eta = [\eta_x, \eta_y, \eta_\psi]^T$ represents the control input vector.

The Coriolis and centripetal forces, $\mathbf{C}_{RB}(\nu_r)\nu_r$ and $\mathbf{C}_A\nu_r$, from Equation (4) are neglected due to the small changes in the body frame when the vessel's velocity is low. Similarly, the damping and current forces, $\mathbf{D}(\kappa, \nu_r)$, can be set to zero because of the small angles involved in low-frequency motion.

2.3.2 Wave-frequency Control Plant Model

To model the wave-frequency (WF) motions, fewer assumptions and simplifications are needed compared to the low-frequency (LF) model. The WF motions can be effectively represented by a harmonic oscillator in state-space form, as shown in Equations (4.7) and (4.8):

$$\dot{\zeta}_w = A_w\zeta_w + E_w w_w \tag{4.7}$$

$$\eta_w = C_w\zeta_w \tag{4.8}$$

Here, $\dot{\zeta}_w$ is the wave-induced motion vector, A_w is the system matrix, E_w is the disturbance matrix, w_w is a zero-mean Gaussian white noise vector, and C_w is the measurement matrix. The matrices are defined mathematically in Equation (4.9):

$$A_w = \begin{bmatrix} \mathbf{0}_{3\times3} & \mathbf{I}_{3\times3} \\ -\Omega^2 & -2\Lambda\Omega \end{bmatrix}, \quad E_w = \begin{bmatrix} \mathbf{0}_{3\times3} \\ K_w \end{bmatrix}, \quad C_w = \begin{bmatrix} \mathbf{0}_{3\times3} & \mathbf{I}_{3\times3} \end{bmatrix} \tag{4.9}$$

Where:

- $\Omega = \text{diag}(\omega_1, \omega_2, \omega_3)$ is the diagonal matrix of natural frequencies.
- $\Lambda = \text{diag}(\zeta_1, \zeta_2, \zeta_3)$ is the diagonal matrix of damping ratios.
- $K_w = \text{diag}(K_{w1}, K_{w2}, K_{w3})$ is the diagonal matrix of wave disturbance gains.

For more detailed explanations and derivations, refer to Sørensen [2018].

2.3.3 Bias Model

The bias model captures the slowly-varying forces and moments caused by second-order wave loads, ocean currents, wind, and any errors in the modeling process. A commonly used bias model is the Markov model, where the bias vector $\mathbf{b} \in R^3$ is governed by the following equation:

$$\dot{\mathbf{b}} = -\mathbf{T}_b^{-1}\mathbf{b} + \mathbf{E}_b\mathbf{w}_b \tag{15}$$

In this equation, $\mathbf{b}$ represents the bias vector, $\mathbf{w}_b$ is a vector of zero-mean Gaussian white noise, $\mathbf{T}_b$ is a diagonal matrix of bias time constants, and $\mathbf{E}_b$ is a diagonal scaling matrix.

An alternative bias model is the Wiener process, which is described by the following equation:

$$\dot{\mathbf{b}} = \mathbf{E}_b\mathbf{w}_b \tag{16}$$

In this model, the bias evolves purely as a stochastic process driven by the noise vector $\mathbf{w}_b$ and scaled by $\mathbf{E}_b$.

2.3.4 Measurements

The measurement equation is given by:

$$\mathbf{y} = \eta + \eta_\omega + \mathbf{v}$$

In this equation, $\mathbf{y}$ represents the output, which is composed of the low-frequency (LF) motion η, the wave-frequency (WF) motion η_ω, and the measurement noise $\mathbf{v} \in R^3$. The noise vector $\mathbf{v}$ is assumed to be zero-mean Gaussian noise.

3 Environmental Loads

Models of environmental loads are essential for achieving realistic simulations of a marine vessel. For Project 1, we will look at only the current and the wind models; in the next project, we will also implement the wave model.

3.1 Current Model

Water currents can behave as disturbances on the vessel and must be taken into account when designing and implementing the controller.

When talking about current modeling, we are looking at two levels of detail:

- Surface current: used for modeling the surface vessel response
- Full current profile: for use in modeling of riser, anchor lines, etc.

A two-dimensional (2D) current model (surface current) is sufficient when modeling a surface vessel, and this approach is described in the following subsection.

3.1.1 Surface currents

For the current velocity vector ν_c in NED frame, we get the following equation:

$$\nu_c = \begin{bmatrix} V_c \cos\psi_c \\ V_c \sin\psi_c \\ 0 \end{bmatrix} \tag{5}$$

Where V_c is the magnitude and ψ_c is the direction in the NED frame. Recall that the down component is zero.

The variation in current velocity, V_c, may be implemented by a first order Gauss-Markov Process,

where ω represents the white noise and the constant $\mu \geq 0$.

$$\omega = \dot{V}_c + \mu V_c$$

Similarly, the variation in current direction, ψ_c, may be implemented as

$$\omega = \dot{\psi}_c + \mu \psi_c$$

3.1.2 Simulink Implementation of the Current Model

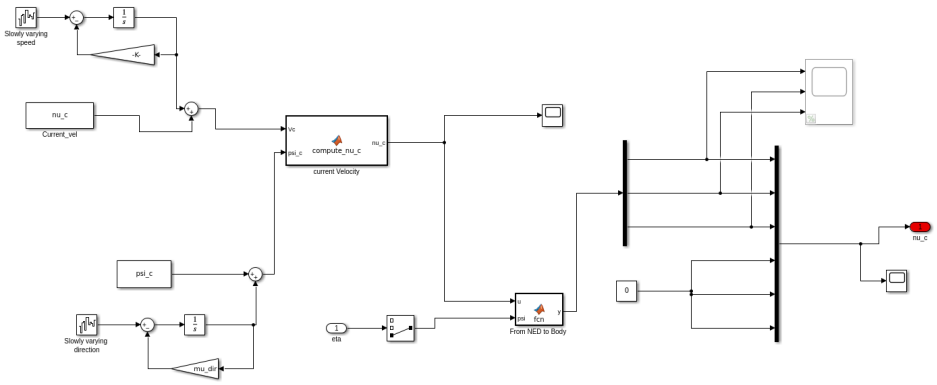

Figure 5: Current Simulink Model

The Simulink represents the current model where both the magnitude and direction of the water current vary over time. The slowly varying current speed and direction are modeled using first-order Gauss-Markov processes. In the model, signal generator blocks provide initial inputs for current speed (V_c) and direction (ψ_c). These inputs pass through integrator blocks ($\frac{1}{s}$) to represent their gradual variation, and a damping factor ($-K$) is applied to account for resistance. The resulting outputs are used as the time-varying current speed and direction. These two signals are then fed into the "compute_nu_c" block, which calculates the current velocity vector (ν_c) in the North-East-Down (NED) frame using the equation:

$$\nu_c = \begin{bmatrix} V_c \cos \psi_c \\ V_c \sin \psi_c \\ 0 \end{bmatrix}$$

Once the current velocity vector is computed, it is transformed from the NED frame to the body-fixed frame (the ship's frame of reference) using the "From NED to Body" transformation block. This transformation takes into account the ship's heading angle (ψ) to accurately convert the velocities. The resulting body-frame velocities are used as feedback for the ship's controller, allowing it to compensate for the disturbances caused by the currents. Additionally, the computed velocities and directions are visualized in the model using scopes and plotting blocks to monitor the system's response. The current model effectively simulates the varying water currents and their impact on the vessel, ensuring realistic behavior for dynamic positioning tasks.

3.2 Wind Model

Wind is the movement of air and is typically divided into two components: a mean value and a fluctuating component (gusts). Although wind forces are often smaller compared to wave and current forces, they cannot be neglected. While wind is inherently a three-dimensional phenomenon, the commonly used models restrict the analysis to horizontal plane velocities, characterized by the wind speed U and direction ψ [6].

In this project, wind loads are computed as generalized forces acting on the body frame across all six degrees of freedom (DOFs). The wind model utilizes a coefficient table, where the generalized wind forces are calculated as:

$$F_{\text{wind}} = |V_w|^2 \cdot C_w\left(\alpha_{rw}\right) \tag{21}$$

Here, F_{wind} represents the generalized wind forces, V_w is the wind velocity magnitude, $C_w(\alpha_{rw})$ is the wind coefficient matrix, and α_{rw} is the relative angle between the wind direction and the vessel heading.

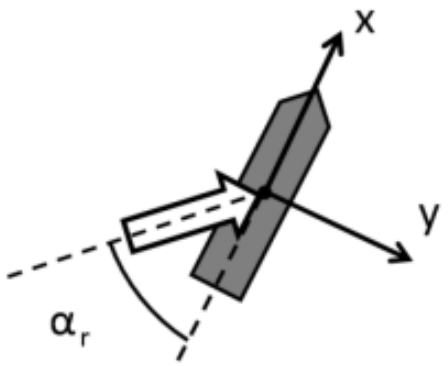

Figure 6: WInd Relative Angle Calculation

Figure 5 shows how the relative wind angle is calculated. The detailed procedure for calculating the relative incidence angle is provided in Appendix A of the project description for part 2.

3.3 Mean Wind Component

The mean wind velocity at elevation z is expressed as:

$$\begin{aligned} \frac{\bar{U}(z)}{\bar{U}_{10}} &= \frac{5}{2}\sqrt{\kappa}\ln\left(\frac{z}{z_0}\right) \\ z_0 &= 10 \times \exp\left(-\frac{2}{5\sqrt{\kappa}}\right) \end{aligned} \tag{22}$$

where $\bar{U}_{10}$ is the one-hour wind speed at an elevation of 10 meters, κ is the sea surface drag coefficient, and z is the elevation.

3.4 Slowly Varying Component

Slowly-varying changes in the mean wind velocity can be modeled using a first-order Gauss-Markov process [6]:

$$\dot{\bar{U}} + \mu \bar{U} = w \tag{23}$$

where w is Gaussian white noise and μ is a constant ($\mu \geq 0$). If $\mu = 0$, the process becomes a random walk. The wind velocity is constrained by saturation limits:

$$0 \leq \bar{U}_{\min} \leq \bar{U} \leq \bar{U}_{\max} \tag{24}$$

Variations in wind direction can be modeled similarly:

$$\dot{\psi} + \mu_2 \psi = \omega_2 \tag{25}$$

$$\psi_{\min} \leq \psi \leq \psi_{\max} \tag{26}$$

where ω_2 is Gaussian white noise, and μ_2 is a positive constant.

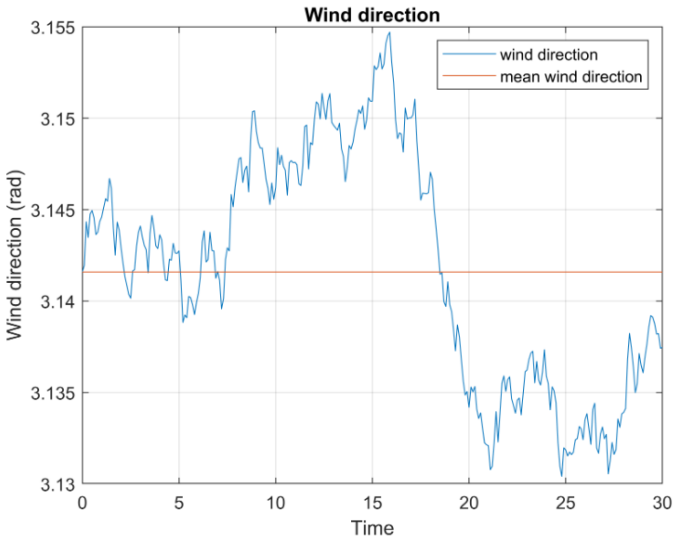

Figure 7: Wind direction variation around mean value

3.5 Simulink Implementation of the Wind Model

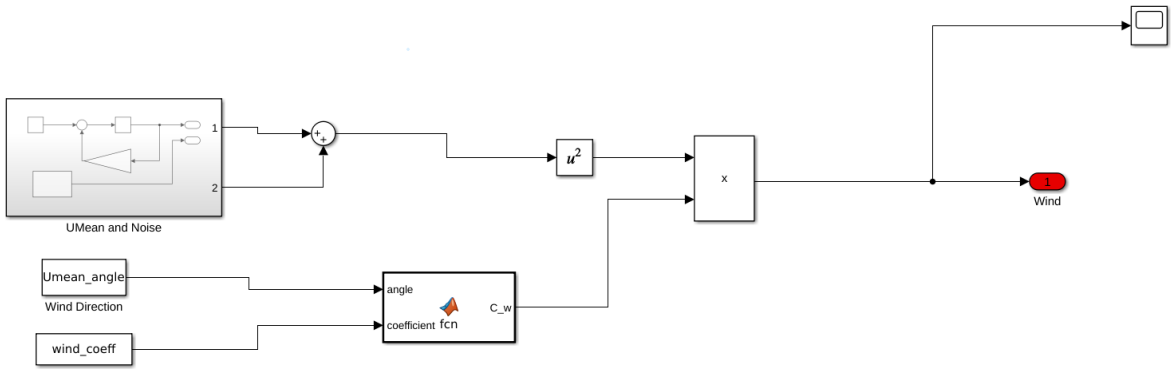

Figure 8: Wind Simulink Model

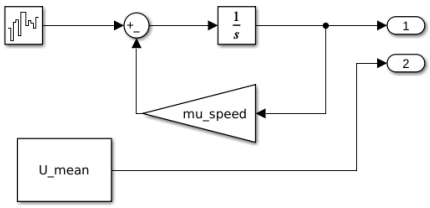

Figure 9: Umean with Noise

The Simulink model for wind includes both the mean wind component and the slowly varying wind fluctuations. In the first block, the mean wind velocity, U_{mean}, and Gaussian white noise are combined to represent the wind disturbances acting on the vessel. The slowly varying component of the wind speed is modeled using a first-order Gauss-Markov process, where white noise is integrated to simulate gradual variations in wind speed. The process is tuned by a parameter, μ_{speed}, which controls the rate of variation. This slowly varying wind speed is summed with the mean wind speed to give a more realistic wind profile over time.

In the second part of the model, the wind forces acting on the vessel are computed based on the relative wind angle, which is determined by the mean wind direction (ψ) and the vessel's heading. The wind coefficient function block uses the wind direction and a wind coefficient table to compute the wind force coefficient, C_w. The generalized wind forces are then computed using the formula:

$$F_{\text{wind}} = |V_w|^2 \cdot C_w(\alpha_{rw})$$

where V_w is the wind velocity and α_{rw} is the relative wind angle. The output of the wind model provides the wind forces that are applied to the body frame of the vessel, which are crucial for the vessel's control system to compensate for disturbances caused by the wind.

4 Reference Model

A reference model is essential for the Dynamic Positioning (DP) control system, as the controller must function in both stationkeeping and trajectory-following modes. When the vessel is required to follow multiple reference points, an autopilot is used. The reference model is implemented in the NED-frame (North-East-Down) and allows us to select a global position.

The reference model is designed to smooth the reference signal and minimize abrupt transitions. This is particularly useful in preventing large, sudden changes in reference signals, such as an immediate shift from 0 to 50 meters, which can destabilize the controller or vessel.

4.1 Implementation of the Reference Model

The chosen reference model is a cascade reference model (see pages 181-182), which combines a first-order low-pass filter with a mass-spring-damper system. The low-pass filter smooths the signal and prevents step changes in the controller's output, while the mass-spring-damper system captures the dynamics necessary for the vessel to follow the trajectory. The reference model is described by the following equations:

$$\mathbf{a}_d^e + \mathbf{\Omega}\mathbf{v}_d^e + \mathbf{\Gamma}\mathbf{x}_d^e = \mathbf{\Gamma}\mathbf{x}_{ref} \tag{25}$$

$$\dot{\mathbf{x}}_{ref} = -\mathbf{A}_f\mathbf{x}_{ref} + \mathbf{A}_f\eta_r \tag{26}$$

The matrices in these equations are defined as:

$$\mathbf{\Omega} = \text{diag}\left\{2\zeta_i\omega_i\right\}, \quad i = 1,2,3 \tag{27}$$

$$\mathbf{\Gamma} = \text{diag}\left\{\omega_i^2\right\}, \quad i = 1,2,3 \tag{28}$$

$$\mathbf{A}_f = \text{diag}\left\{\frac{1}{t_i}\right\}, \quad i = 1,2,3 \tag{29}$$

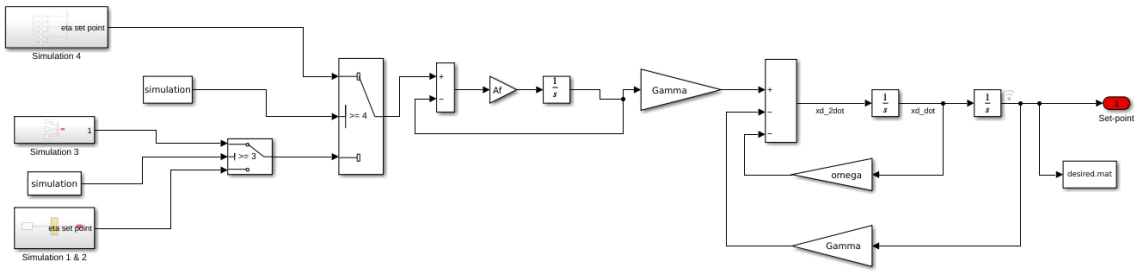

Figure 10: Simulink Reference Model

The Simulink implementation of the reference model is essential for ensuring smooth and stable performance of the Dynamic Positioning (DP) control system. The model is designed to provide reference signals for both stationkeeping and trajectory-following modes. To achieve this, the reference signal is processed using a cascade reference model, which combines a low-pass filter and a mass-spring-damper system. This setup ensures that sudden changes in the reference signals, such as abrupt position shifts, are filtered, preventing destabilization of the vessel or controller.

The reference model begins by inputting the desired reference set points. Depending on the simulation scenario, the model checks which set point to use. The chosen set point then passes through a low-pass filter (represented by the integrator and Af blocks) to ensure smooth transitions. The mass-spring-damper system, represented by the Gamma and Omega blocks, is responsible for adding necessary

dynamics that enable the vessel to follow the reference trajectory. The output of the model provides smoothed reference signals for position and velocity (xd_dot and xd_2dot) in the NED frame. These reference signals are then fed into the control system to guide the vessel's movement toward the desired set points in a controlled and stable manner.

4.2 Tuning of the Reference Model

The reference model is tuned by observing each position trajectory and comparing it with the input reference trajectory. To avoid oscillations, the damping coefficient ζ_i is adjusted to achieve either critical or over-damping. For a critically damped system, $\zeta = 1$, and for an over-damped system, $\zeta > 1$. Initially, ζ_i is set to 1, and increased if oscillations are observed. This tuning is performed for each state individually, and adjustments to the controller are made if necessary.

The natural period corresponding to ω_i typically ranges from 50 to 200 seconds for vessels of this size. Initially, ω_i is set using the relation $\omega_i = \frac{2\zeta_i 2\pi}{T}$, where T is the desired period in seconds. For this system, the period is chosen as $T = 10$ seconds, giving an initial value of $\omega_i = \frac{2\pi}{10}$ for each state. The values of ω_i are adjusted during tuning to ensure the best system response.

The filter gain $\mathbf{A_f} = [0.1, 0.1, 0.01]$ is applied to the system to smoothen the response, reducing the impact of high-frequency disturbances. The time constant for the low-pass filter is set such that the filter reaches 63.2% of its maximum value at time t_i for each state.

i	t_i (s)	ζ_i	ω_i
1	20	1.0	$\frac{2\pi}{10}$
2	20	1.0	$\frac{2\pi}{10}$
3	20	1.0	$\frac{2\pi}{10}$

Table 1: Final tuning parameters for the reference model

The damping ratio is set to $\zeta_i = 1$ for all states to ensure critical damping. The natural frequency ω_i is initially set to $\frac{2\pi}{10}$, corresponding to a period of 10 seconds, and adjusted as needed based on system performance.

5 Trust Allocation

The control algorithm outputs the total forces and moments required to move the vessel to the desired reference point. However, these forces cannot be directly applied to the ship, as there is no way to distribute the generalized forces to its individual thrusters. Therefore, we need to implement a thrust allocation system that decomposes the generalized forces calculated by the PID controller into individual commands for each thruster. This process is known as Thrust Allocation.

Since the system is over-actuated, several approaches are possible for thrust allocation. An extended thrust alloInitially, a quadratic programming-based optimization approach was considered, but it was abandoned in favor of focusing on report writing and overall system tuning. Instead, a simple yet effective thrust allocation algorithm was used.

5.1 Thrusters

The supply vessel is equipped with five thrusters: one tunnel thruster located at the bow, and four azimuth thrusters. Two are positioned at the stern and two at the bow.

As with any physical system, the thrusters are subject to limitations, such as maximum thrust, thrust ramp rate, and the rotation rate of the azimuth thrusters. Table 8.1 outlines the key specifications and limitations for each thruster. Thrusters 2, 4, and 5 are azimuth thrusters that can rotate freely.

Thruster Number	Position X [m]	Position Y [m]	Angle [deg]
1	39.3	0	90
2	35.6	0	α_2
3	31.3	0	90
4	-28.5	5	α_4
5	-28.5	-5	α_5

Table 2: Thruster positions and angles.

5.2 Linear Effector Model

The relationship between the thrust exerted by the actuators and the generalized forces is described by the Linear Effector Model (Eq. 8.1):

$$\boldsymbol{\tau} = \mathbf{B}u \tag{8.1}$$

Here, $\boldsymbol{\tau}$ is the vector of generalized forces, $\boldsymbol{u}$ is the vector of thruster commands, and $\mathbf{B} \in R^{m \times p}$ is the effectiveness matrix that describes how the thrusters generate the forces $\boldsymbol{\tau}$. In this case, $p = 5$ represents the number of thrusters, and $m = 3$ corresponds to the degrees of freedom (surge, sway, and yaw).

To allocate thrust, we need to compute the inverse of the matrix $\mathbf{B}$, or more practically, its pseudo-inverse, since $\mathbf{B}$ is generally not square. The thruster commands can then be computed as:

$$\boldsymbol{u} = \mathbf{B}^{-1}\boldsymbol{\tau} \tag{8.2}$$

The vector $\boldsymbol{u}$ is given by:

$$\boldsymbol{u} = \begin{bmatrix} u_1 & u_2 & u_3 & u_4 & u_5 \end{bmatrix}^T \tag{8.3}$$

Each thruster's contribution to the forces is described in the $\mathbf{B}$ matrix. The tunnel thruster generates forces only in the sway direction, with a corresponding moment in yaw, as shown in Eq. 8.4:

$$b_1 = \begin{bmatrix} 0 & 1 & l_{x,1} \end{bmatrix}^T \tag{8.4}$$

Azimuth thrusters generate both surge and sway forces, as well as moments. The forces depend on the angular position of the thruster, and they are expressed as body-fixed forces in Eq. 8.5:

$$b_i = \begin{bmatrix} \cos(\alpha_i) & \sin(\alpha_i) & l_{x,i}\sin(\alpha_i) - l_{y,i}\cos(\alpha_i) \end{bmatrix}^T, \quad i = \{2,3,4,5\} \tag{8.5}$$

Thus, the full $\mathbf{B}$ matrix is:

$$\mathbf{B} = \begin{bmatrix} 0 & \cos(\alpha_2) & 0 & \cos(\alpha_4) & \cos(\alpha_5) \\ 1 & \sin(\alpha_2) & 1 & \sin(\alpha_4) & \sin(\alpha_5) \\ l_{x,1} & l_{x,2}\sin(\alpha_2) - l_{y,2}\cos(\alpha_2) & l_{x,3} & l_{x,4}\sin(\alpha_4) - l_{y,4}\cos(\alpha_4) & l_{x,5}\sin(\alpha_5) - l_{y,5}\cos(\alpha_5) \end{bmatrix} \tag{8.6}$$

The expanded form of Eq. 8.1 for our vessel is:

$$\begin{bmatrix} F_X \\ F_Y \\ M \end{bmatrix} = \begin{bmatrix} 0 & \cos(\alpha_2) & 0 & \cos(\alpha_4) & \cos(\alpha_5) \\ 1 & \sin(\alpha_2) & 1 & \sin(\alpha_4) & \sin(\alpha_5) \\ 39.5 & 35.3\sin(\alpha_2) & 31.3 & -28.5\sin(\alpha_4) - 5\cos(\alpha_4) & -28.5\sin(\alpha_5) + 5\sin(\alpha_5) \end{bmatrix} \begin{bmatrix} u_1 \\ u_2 \\ u_3 \\ u_4 \\ u_5 \end{bmatrix} \tag{8.7}$$

8.3 Extended Thrust Approach

In Equation (8.7), the effectiveness matrix $\mathbf{B}$ depends on the thruster angles $\boldsymbol{\alpha}$. This creates a challenge because the thruster angles are variables we aim to compute in the thrust allocation algorithm, rather than known inputs. To address this, we adopt an extended thrust approach. In this method, we decompose the control inputs for the azimuth thrusters into longitudinal and lateral components and treat each component as a separate thruster.

Figure 8.1: Decomposition of azimuth thrust

The extended thrust vector is then expressed as:

$$\boldsymbol{u}_{\text{exp}} = [\boldsymbol{u}_1, \boldsymbol{u}_{2,x}, \boldsymbol{u}_{2,y}, \boldsymbol{u}_3, \boldsymbol{u}_{4,x}, \boldsymbol{u}_{4,y}, \boldsymbol{u}_{5,x}, \boldsymbol{u}_{5,y}]^T \tag{8.8}$$

$$= [\boldsymbol{u}_1, \boldsymbol{u}_2, \boldsymbol{u}_3, \boldsymbol{u}_4, \boldsymbol{u}_5, \boldsymbol{u}_6, \boldsymbol{u}_7, \boldsymbol{u}_8]^T \tag{8.9}$$

The $\mathbf{B}$ matrix must also be expanded. Each x-component contributes to surge and moment, while each y-component affects sway and moment. The components are given by:

$$b_i = [0, 1, l_{x,i}]^T, \quad i = \{1,2,4,6,8\}$$
$$b_i = [1, 0, l_{y,i}]^T, \quad i = \{3,5,7,9\}$$

This results in the expanded $\mathbf{B}$ matrix for the system:

$$\mathbf{B} = \begin{bmatrix} 0 & 1 & 0 & 0 & 1 & 0 & 1 & 0 \\ 1 & 0 & 1 & 1 & 0 & 1 & 0 & 1 \\ 39.3 & 0 & 35.6 & 31.3 & -5 & -28.5 & -5 & -28.5 \end{bmatrix} \tag{8.10}$$

$$\Rightarrow \begin{bmatrix} F_X \\ F_Y \\ M \end{bmatrix} = \begin{bmatrix} 0 & 1 & 0 & 0 & 1 & 0 & 1 & 0 \\ 1 & 0 & 1 & 1 & 0 & 1 & 0 & 1 \\ 39.3 & 0 & 35.6 & 31.3 & -5 & -28.5 & -5 & -28.5 \end{bmatrix} \begin{bmatrix} u_1 \\ u_2 \\ u_3 \\ u_4 \\ u_5 \\ u_6 \\ u_7 \\ u_8 \end{bmatrix} \tag{8.11}$$

5.3 Simulink Implementation of the Thrust Allocations

The Simulink implementation of the thrust allocation system is shown in the figure. The control system computes the total forces and moments needed to achieve the desired motion of the vessel, represented by the generalized forces vector, τ_d. However, these forces need to be distributed among the individual thrusters on the vessel. The thrust allocation system performs this task by solving a quadratic programming (QP) problem to minimize the thrust usage while adhering to the physical constraints of the thrusters.

The Simulink block contains a MATLAB Function block, which takes in the desired forces, τ_d, and the thruster effectiveness matrix, $\mathbf{B}$. Inside the MATLAB function, a quadratic programming problem is formulated to compute the thrust commands for each thruster. The function uses the 'quadprog' solver to minimize the thrust while ensuring that the forces generated by the thrusters match the required forces, τ_d. The resulting thrust magnitudes and angles are then passed to the output of the block, where u represents the thrust magnitudes and α represents the azimuth angles for the rotatable thrusters.

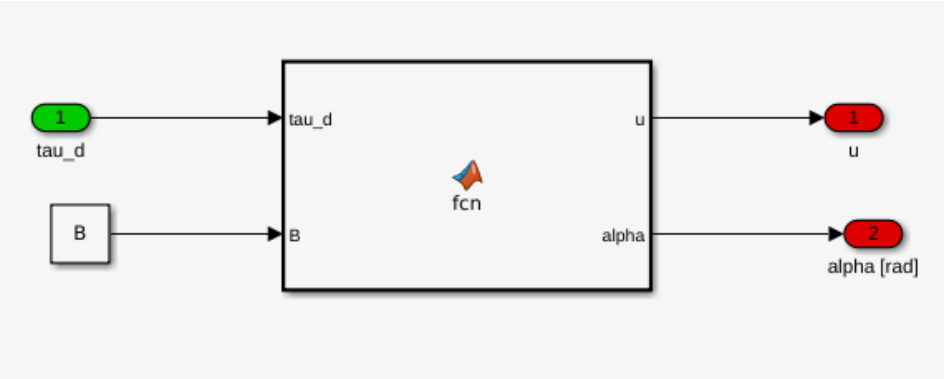

Figure 11: Thrust Allocation Block

This implementation effectively handles the over-actuation of the vessel by optimizing the allocation of thrust across multiple thrusters. The quadratic programming approach ensures that the allocation is optimal, minimizing unnecessary thrust usage while meeting the control demands.

6 Controller Design

The controller's main objective is to align the state variables with the desired setpoints using a feedback loop. It compares the system's current state with the desired state and generates an input to reduce the error.

In this case, the controller receives a target trajectory from the reference model, as well as the current state variables—surge, sway, yaw, and their rates of change. Based on this, the controller produces a control input τ, which is applied to the ship model after adjusting for the reference frame.

The desired Earth-fixed position and velocity are represented by η_d and ν_d, respectively. Each term in the control law involves a diagonal gain matrix and an error term, with the goal of minimizing the error $e(t)$, defined as the difference between the desired position $y_0(t)$ and the current position $y(t)$.

6.1 Proportional-Integral-Derivative (PID) Control

The PID controller, although a straightforward solution to the Dynamic Positioning (DP) challenge, provides a reliable and robust method. Its ease of implementation, widespread use in various fields, and efficiency make it a strong candidate for the DP control system. Each term in the PID controller serves a vital function: the integral term corrects steady-state errors, defined as $e_\infty = \eta_{d\infty} - \eta_\infty$, while the derivative term helps introduce damping into the system to stabilize the response.

The controller is expressed in Eq. 50, in a reduced vector form:

$$\tau^{(b)}(1,2,6) = \begin{bmatrix} \tau_u \\ \tau_v \\ \tau_\psi \end{bmatrix} = R^T(\psi)\tau^n = R^T(\psi)\left[K_p e - K_d\dot{\eta} + K_i \int_0^\infty e(x)dx\right] \tag{50}$$

Here, the vector $\tau^{(b)}$ is reduced from a 6×1 to a 3×1 vector based on the assumption that roll, pitch, and heave motions are already stabilized and remain constant (set to zero) within the DP controller block, as shown in Figure 18.

The error between the desired position η_d and the current position η is defined as:

$$e = \eta_d - \eta$$

The derivative of the position vector η is expressed as:

$$\dot{\eta} = R(\psi)\nu = \begin{bmatrix} \dot{x} & \dot{y} & \dot{z} & \dot{\phi} & \dot{\theta} & \dot{\psi} \end{bmatrix}^T$$

The controller gains, denoted by K_j, where j represents the proportional (p), integral (i), and derivative (d) terms, are structured as diagonal matrices:

$$K_j = \begin{bmatrix} K_{ju} & 0 & 0 \\ 0 & K_{jv} & 0 \\ 0 & 0 & K_{jr} \end{bmatrix}$$

The implementation of the DP controller along with its corresponding PID controller was carried out

in Simulink, as illustrated in Figures 18 and 19.

Proportional Term: The proportional term is the product of the proportional gain and the error. It dictates the speed of the controller's response. A high proportional gain may lead to instability, while a low gain results in slow responses. Using only the proportional term can cause the vessel to never fully reach the setpoint due to steady-state error, which can be corrected by adding the integral term.

Integral Term: The integral term corrects steady-state error by accumulating the error over time. However, if the integral gain is too large, it may cause overshooting or instability (integral windup), leading to oscillations.

Derivative Term: The derivative term predicts future errors based on the current rate of change. A high rate of error change results in a larger output, leading to faster controller responses. However, rapid small fluctuations can be problematic and are often mitigated with an input filter.

6.2 Implimentation of the PID Controller

The Simulink implementation of the Proportional-Integral-Derivative (PID) controller for the Dynamic Positioning (DP) system is shown in the figure. The PID controller calculates the control input, τ (in the body frame), to adjust the vessel's position and heading according to the desired setpoints. The controller uses the error between the desired position, $\eta_{\text{set point}}$, and the current position, η, which is processed in the NED to body frame transformation block to account for the vessel's orientation (yaw, ψ). The error is then used to compute the PID terms.

The proportional term, K_p, corrects the error based on its current magnitude. The integral term, K_i, accumulates the error over time to remove any steady-state error, while the derivative term, K_d, helps stabilize the system by counteracting rapid changes in the error signal. The integral and derivative actions are applied using the integrator and gain blocks. The outputs of the proportional, integral, and derivative terms are summed together to produce the control signal, τ, which is then sent to the vessel to adjust its motion in the body frame.

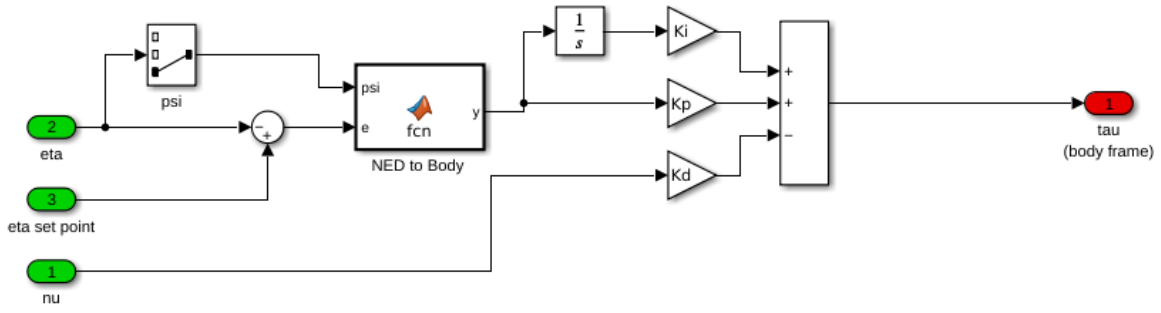

Figure 12: PID Controller Block

The PID controller provides a straightforward yet robust solution for dynamic positioning. By adjusting the gains, K_p, K_i, and K_d, the system can be tuned to achieve the desired balance between

responsiveness and stability. The proportional gain ensures a quick reaction to the error, while the integral term eliminates steady-state offsets. The derivative term further smooths the response by damping rapid changes in the error, preventing overshooting or oscillations.

6.3 Tunning of the PID

The controller was tuned using a modified Ziegler-Nichols approach to ensure system stability, with all poles having negative real parts. Initially, the proportional gains were increased until oscillations in η appeared, and then slightly reduced. The derivative term was adjusted to add damping and smooth the system's response. Lastly, the integral gains were fine-tuned to eliminate any remaining steady-state error.

After the initial tuning, further adjustments were made to speed up the response and prevent overshooting. The system initially exhibited slow and inverse responses, suggesting the presence of a positive zero and a near-zero pole, which contributed to the sluggish behavior. The system's poles were derived using:

$$\frac{e}{u}(s) = \frac{s}{s^2 + \frac{K_p}{K_d}s + \frac{K_i}{K_d}} \tag{51}$$

The poles, which must have negative real parts, were calculated as:

$$\lambda_{1,2} = -\frac{K_p}{K_d} \pm \sqrt{\left(\frac{K_p}{K_d}\right)^2 - 4\frac{K_i}{K_d}} \tag{52}$$

After correcting for these issues, the final PID gains were determined as follows:

	Surge	Sway	Yaw
K_p	$2.767 \cdot 10^5$	$3.363 \cdot 10^5$	$1.499 \cdot 10^8$
K_i	$1.391 \cdot 10^4$	$1.6905 \cdot 10^4$	$7.535 \cdot 10^6$
K_d	$1.6463 \cdot 10^6$	$1.049 \cdot 10^6$	$5.615 \cdot 10^8$

Table 3: Final PID controller gains

7 Simulation Results

7.1 Simulation 1

Scenario

This simulation tests the DP system's performance under two different environmental conditions. First, the vessel is subjected to a current of $0.5\,[\mathrm{m/s}]$ coming from the east, and in the second case, a wind with an average speed of $10\,[\mathrm{m/s}]$ from the south is applied. The DP setpoint is set to $[0, 0, 0]$, and the vessel's position and heading are plotted until steady state is reached for both cases. The results are presented as individual time-series plots and combined xy-plots for each scenario.

7.1.1 Simulation 1A - Current set to $0.5[\ \mathrm{m/s}]$ from east.

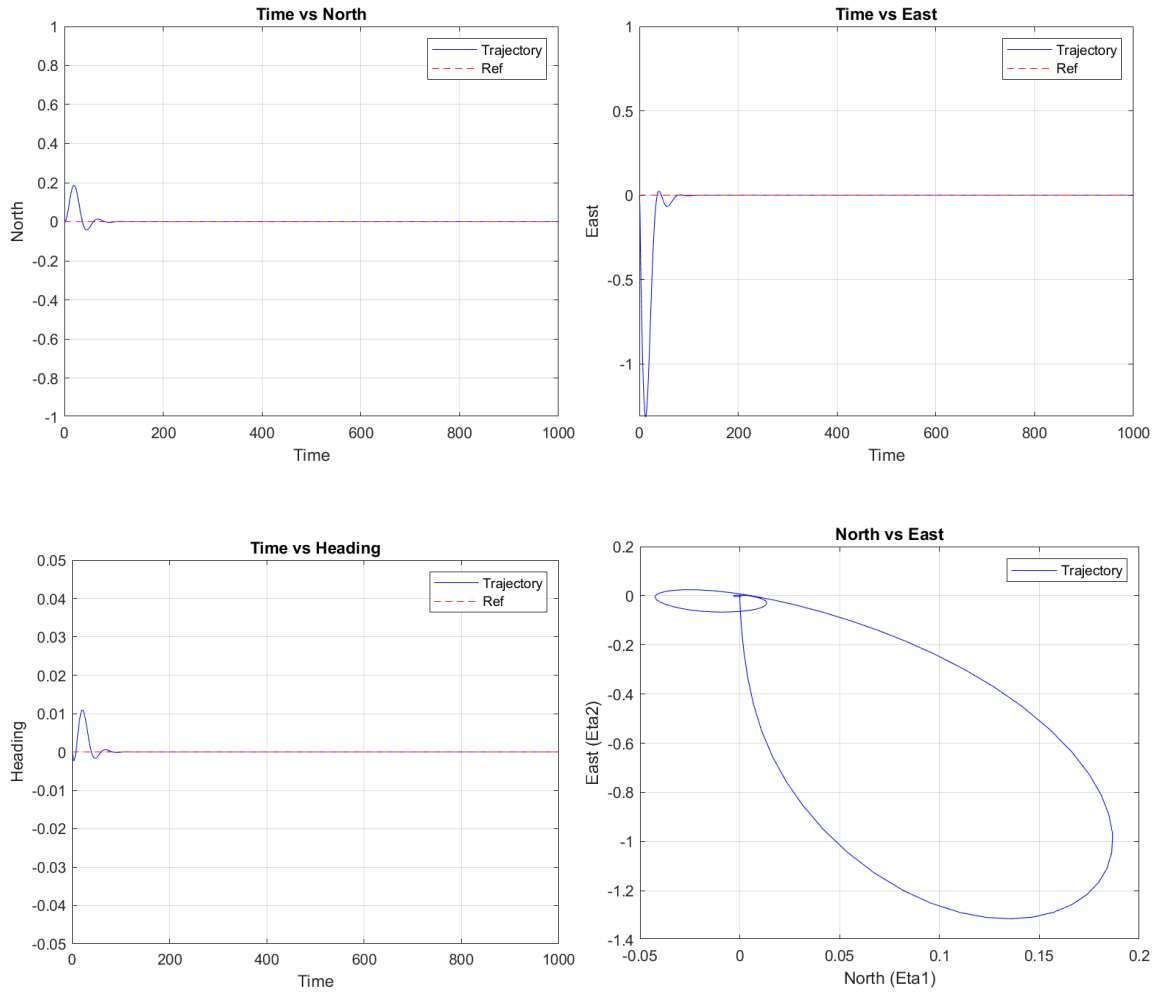

Figure 13: Simulation 1a Results

7.1.2 Discussion

The results from Simulation 1A, where the vessel is subjected to a current of $0.5\,[\mathrm{m/s}]$ from the east, show the Dynamic Positioning (DP) system's ability to effectively correct for environmental disturbances. The North vs Time and East vs Time plots indicate that the vessel experiences initial deviations due to the current's influence, with oscillations observed in both the North and East directions. The eastward current causes the vessel to drift significantly in the East direction initially, while the North direction shows smaller deviations. However, over time, the DP system adjusts, and the vessel converges back to the desired setpoint of $[0, 0]$ with minimal steady-state error. This indicates that the controller is able to manage the current-induced drift effectively, although the system experiences some initial oscillations before stabilizing.

The Heading vs Time plot shows that the vessel's heading also experiences minor oscillations at the start, but these are quickly dampened as the system stabilizes. The North vs East plot provides a clear visualization of the vessel's trajectory, where the initial drift forms an elliptical path before the vessel converges back to the setpoint. The overall trajectory demonstrates the DP system's ability to handle disturbances and return the vessel to its target position and orientation. While the system performs

well in mitigating the effects of the eastward current, the initial response could likely be improved with further tuning of the PID controller to reduce the oscillations and time to steady-state.

7.1.3 Simulation 1B - Wind with average speed of 10[m/s] from south.

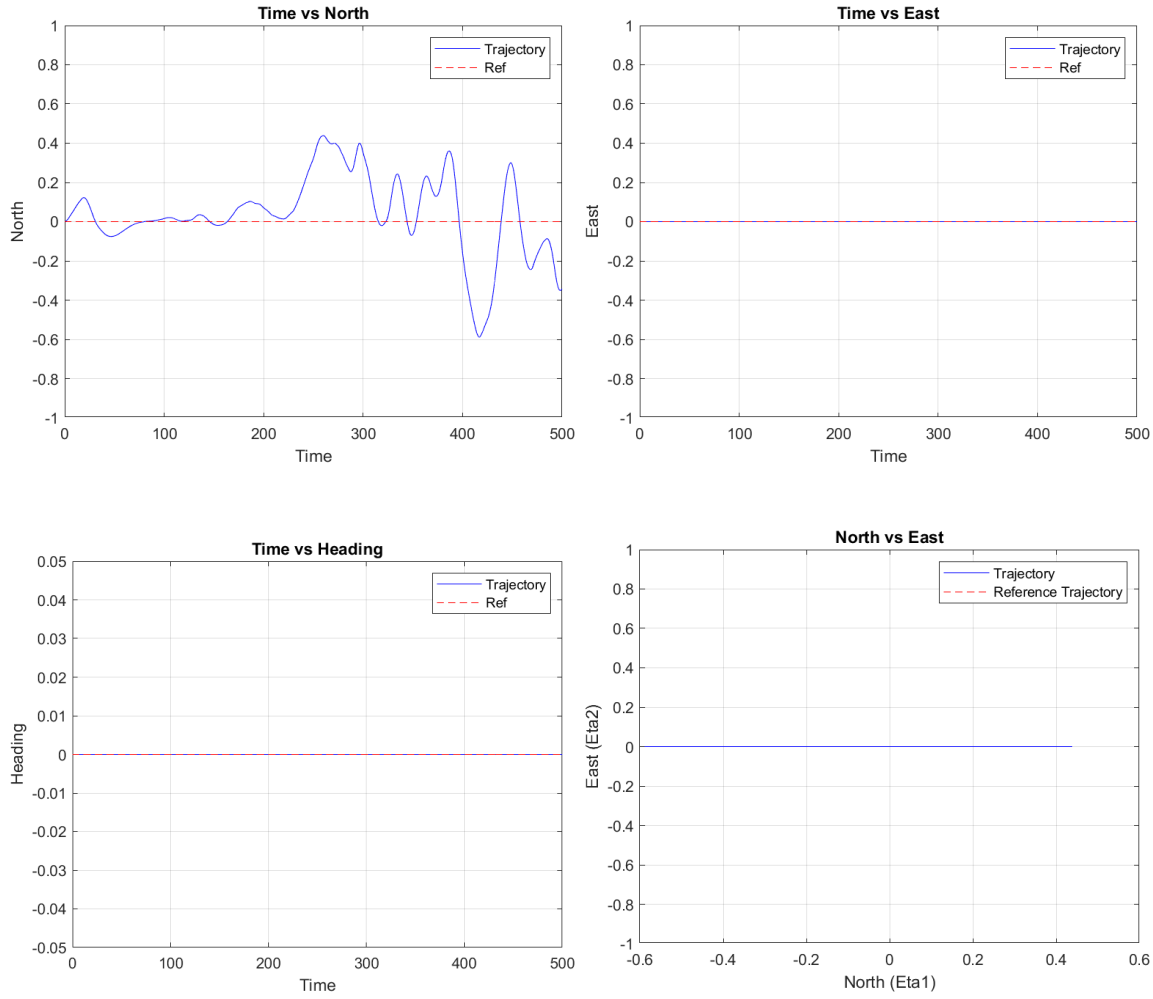

Figure 14: SImulation 1b Results

7.1.4 Discussion

In Simulation 1B, the vessel is subjected to a wind with an average speed of 10 [m/s] from the south. The Time vs North plot reveals that the vessel experiences significant oscillations in the North direction due to the wind, indicating that the DP system struggles to maintain a steady position in the presence of the wind. The oscillations persist throughout the simulation period, and the vessel does not fully stabilize around the setpoint in the North direction. This suggests that the controller may need further tuning to improve its performance under wind disturbances. In contrast, the Time vs East plot shows that the vessel maintains its position along the East axis, with no significant deviations observed. This implies that the wind from the south primarily affects the North direction.

The Time vs Heading plot shows that the vessel's heading remains stable throughout the simulation, closely tracking the reference value with no oscillations, indicating that the DP system successfully

maintains the correct orientation. The North vs East plot provides a visual representation of the vessel's trajectory, showing that the vessel remains largely in place along the East axis, but it experiences substantial fluctuations in the North direction due to the wind. Overall, while the DP system manages to maintain the vessel's heading and East position, the performance in the North direction could be improved with further tuning to better counteract the wind disturbances.

7.2 Simulation 2

In this simulation, wind loads are turned off, and the current varies linearly from 0.5 [m/s] over a 300-second period, gradually changing direction. The current starts flowing from the south at 180° and shifts clockwise to the west at 270° over a period of 200 seconds. The simulation is extended beyond this time until the vessel reaches a steady state, at which point the vessel's position and heading are plotted over time. These data provide insight into the vessel's response to varying currents and its ability to stabilize under such conditions.

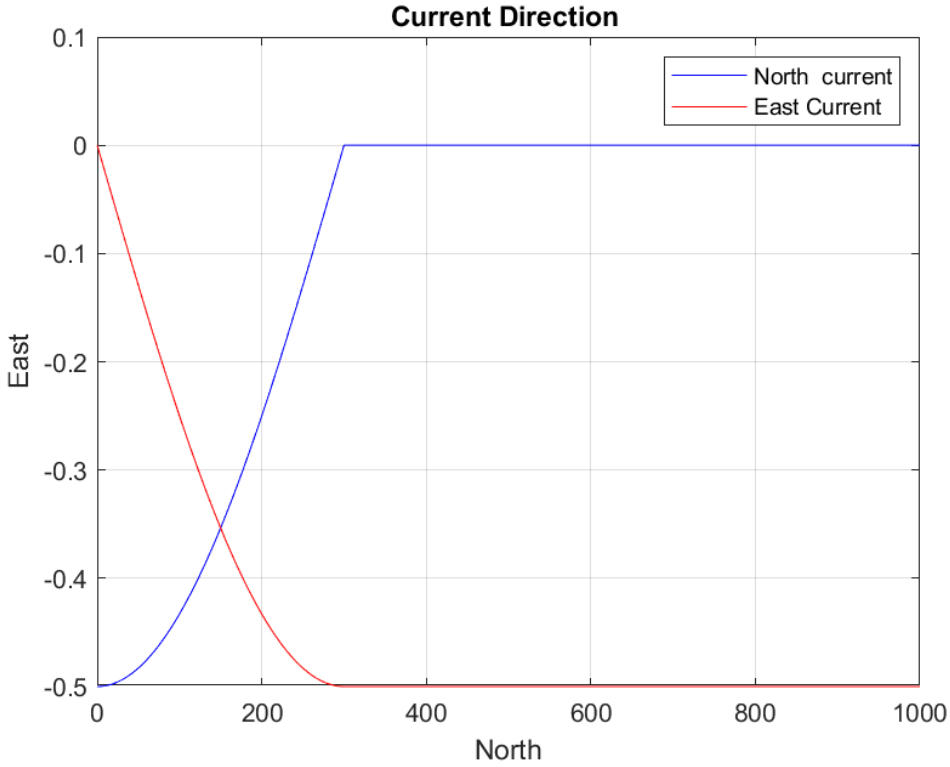

Figure 15: Change of *North* and *East* current components over time as the current direction varies from 180° to 270° over a 200-second period.

Figure 15 illustrates how the current's direction shifts from 180° to 270° over a period of 200 seconds, affecting both the *North* and *East* current components. As seen in Figure 15, the vessel's trajectory is influenced by these changes, transitioning to a steady-state condition where it can compensate for the varying current and maintain stability.

7.2.1 Simulation 2 - current vary linearly from $0.5[\ \mathrm{m/s}]$ coming from North to 0.5 [m/s] coming from East, while keeping the vessel at the origin [0 0 0].

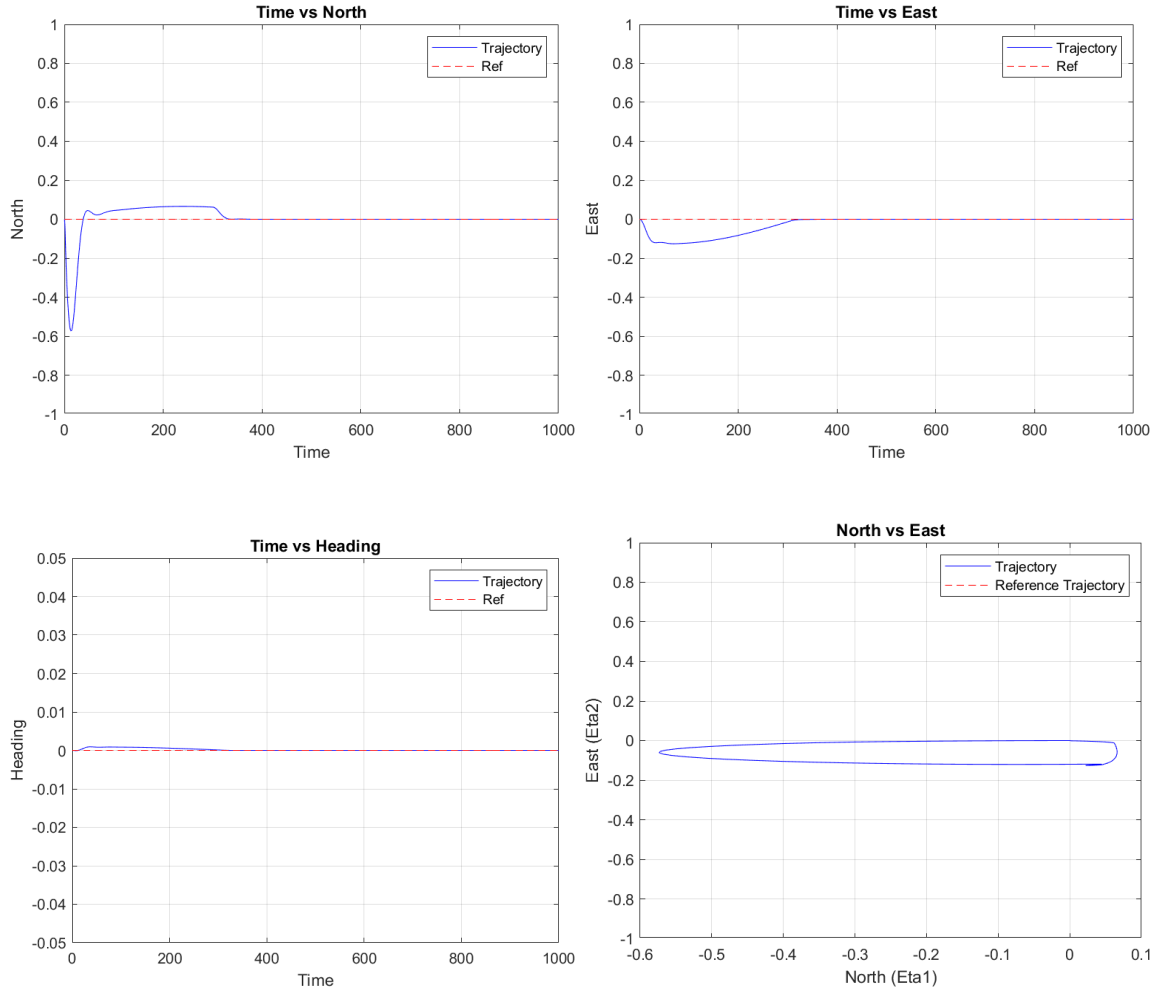

Figure 16: Simulation 2 Results

7.2.2 Discussion

In Simulation 2, the vessel is subjected to a gradually changing current, which varies linearly from 0.5 [m/s] coming from the North to 0.5 [m/s] coming from the East over a period of 300 seconds. The Time vs North plot shows that the vessel initially experiences a deviation from the setpoint, but the DP system compensates for the current and brings the vessel back to the desired position. The Northward deviation is noticeable at the start, but the system manages to stabilize the vessel and return it to the reference point. Similarly, in the Time vs East plot, the vessel also experiences a minor deviation in the East direction, but it quickly stabilizes as the current changes direction from North to East, showing the DP system's ability to counteract the varying current forces.

The Time vs Heading plot indicates that the vessel's heading remains relatively stable throughout the simulation, with only minor oscillations at the beginning as the current starts to change direction. The North vs East plot illustrates the vessel's trajectory in the xy-plane, where the initial deviation is corrected, and the vessel returns to the origin. The trajectory shows an elliptical path as the current shifts direction, but the DP system successfully maintains control, bringing the vessel back

to the reference setpoint. Overall, the DP system performs well in managing the varying current, demonstrating its robustness in keeping the vessel at the origin despite the gradually changing current forces.

7.3 Simulation 3

Scenario

This test compares the vessel's position and heading over time for two cases: one with a reference model and one without. The initial position is set to $\eta_0 = [0, 0]$, and the setpoint is $\eta_{\text{SP}} = \left[10, 10, \frac{3\pi}{2}\right]$. No environmental forces are applied, and the results are shown until the vessel reaches steady state, with the desired trajectory plotted in each case. If the reference model contains velocity trajectories, these are also plotted.

Simulation 3 - Comparing the different results for the vessel position over time for initial position $\eta_0 = \begin{bmatrix} 0 & 0 \end{bmatrix}$ and setpoint $\eta_{\text{SP}} = \begin{bmatrix} 10 & 10 & \frac{3\pi}{2} \end{bmatrix}$, with and without a reference model.

7.3.1 Vessel Dynamics Without Reference Model

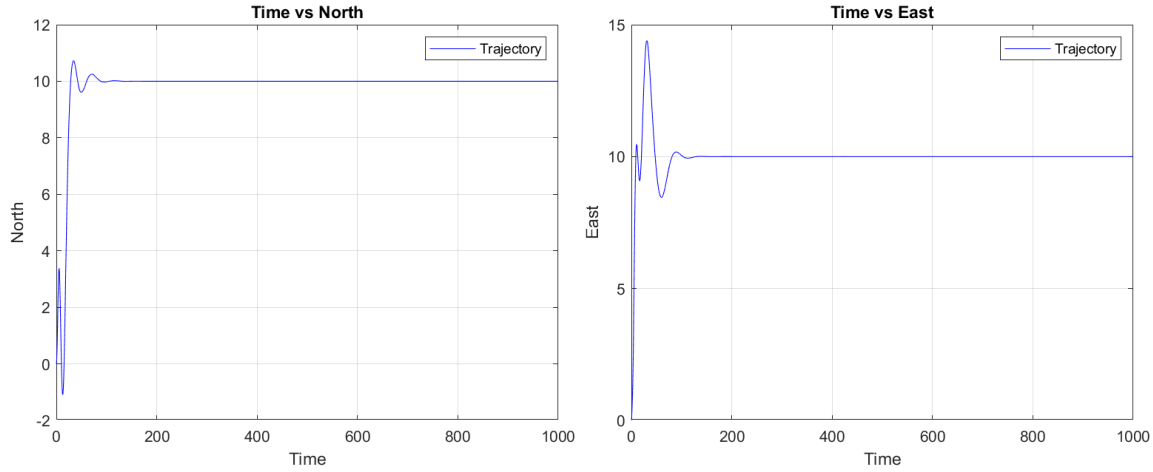

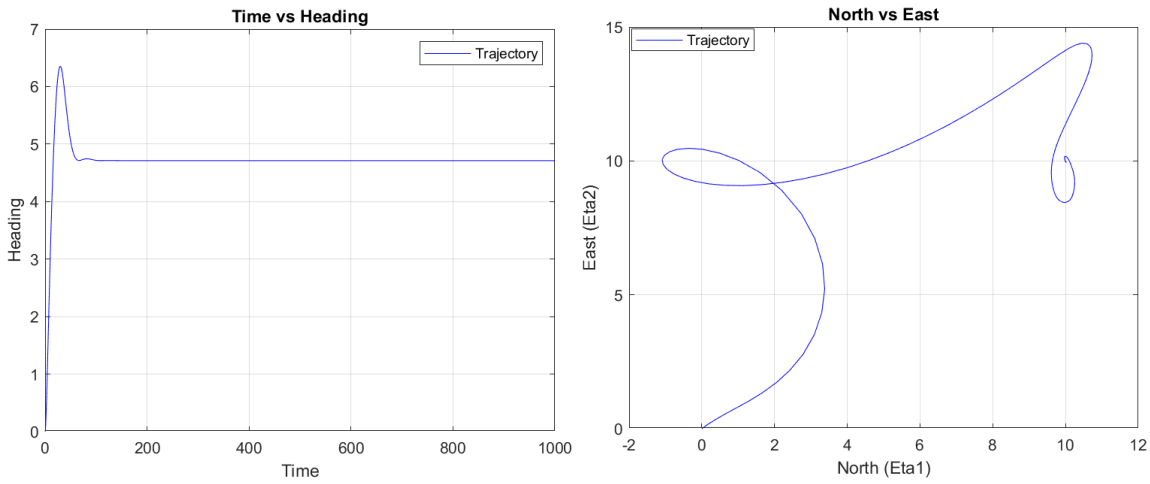

Figure 17: Simulation 3 Results (Without reference model)

7.3.2 Vessel Dynamics With Reference Model

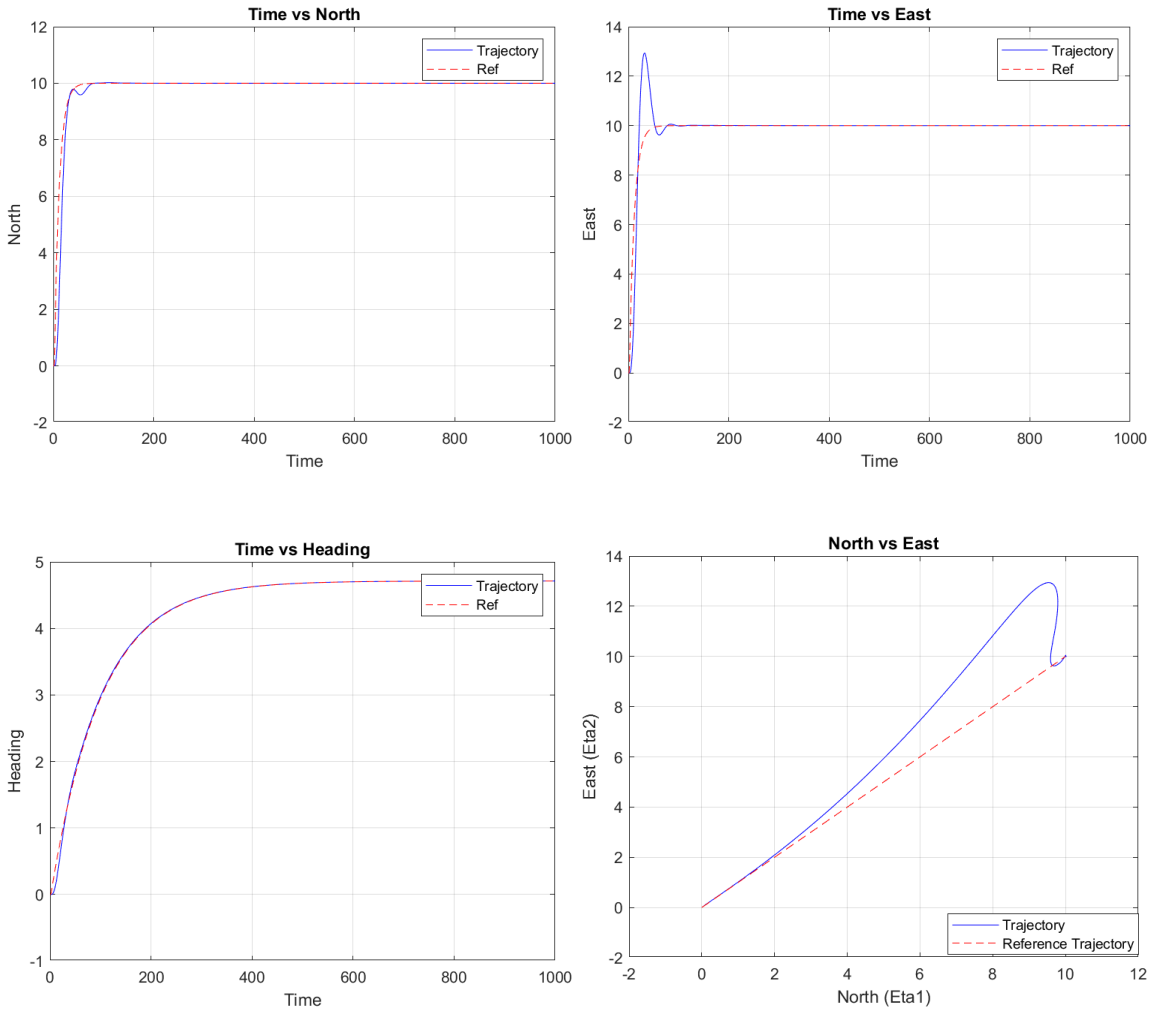

Figure 18: Simulation 3 Results (With reference model)

7.3.3 Discussion

In Simulation 3, the vessel dynamics are compared with and without the use of a reference model. The plots for the vessel dynamics **with the reference model** show that the vessel follows the desired trajectory quite closely, as evidenced by the Time vs North, Time vs East, and Time vs Heading plots. The North and East positions converge to the setpoint of $[10, 10]$, and the heading reaches the desired angle of $\frac{3\pi}{2}$. There are some minor oscillations at the start, especially in the East position, but the vessel stabilizes quickly. The North vs East plot confirms that the trajectory follows the desired path in a controlled manner, with the vessel reaching the setpoint smoothly. The use of the reference model effectively minimizes overshoot and helps smooth the transition to the final position.

In contrast, the plots **without the reference model** reveal a less controlled response. The Time vs North and Time vs East plots show significant oscillations during the initial phase, and while the vessel eventually stabilizes near the setpoint, the response is much less smooth. The Time vs Heading plot shows an initial spike in the heading, followed by a slower convergence compared to the case with the reference model. The North vs East plot shows a more erratic trajectory, with the vessel looping before reaching the setpoint, indicating that the control system struggles to guide the vessel smoothly without the reference model. Overall, the results demonstrate that the reference model helps achieve smoother and more accurate vessel dynamics, particularly in minimizing oscillations and overshooting during the transition to the setpoint.

7.4 Reference Model Velocity Trajectories

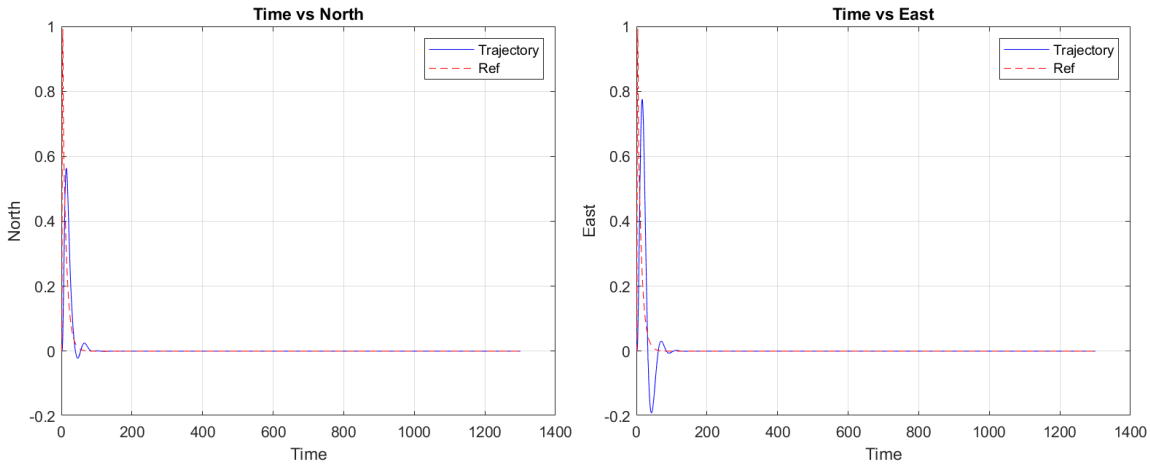

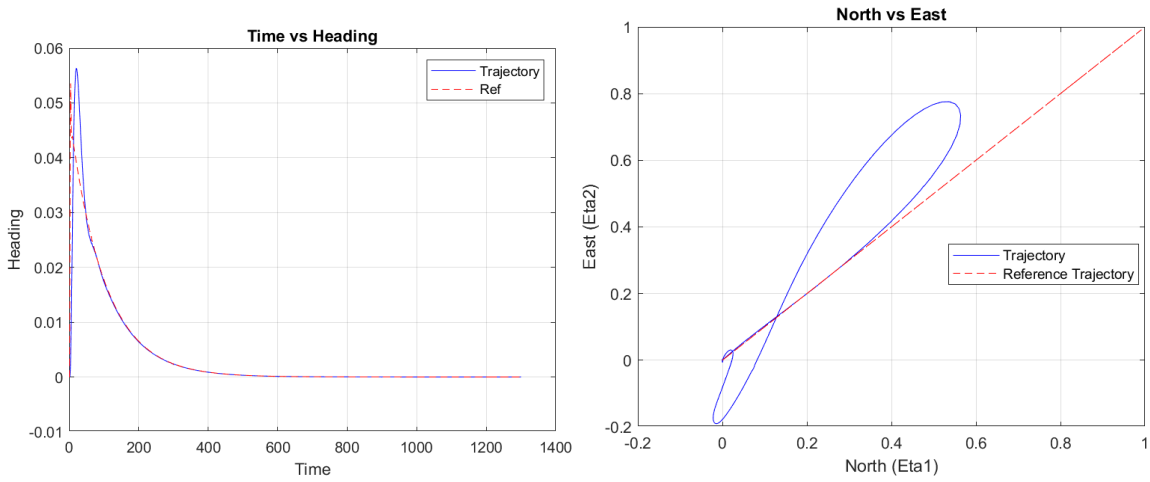

Figure 19: Simulation 3 Velocity Trajectories

7.4.1 Discussion

The velocity trajectories in Simulation 3, as shown in Figure 18, illustrate the vessel's movement towards the desired setpoint. The Time vs North, Time vs East, and Time vs Heading plots show that the velocities in the North, East, and heading directions converge to zero as the vessel stabilizes at the desired position and heading. Initially, there are small fluctuations as the system reacts to the reference velocity commands, but the system quickly dampens these fluctuations, bringing the velocities to a stable state near zero. The North vs East plot highlights the path taken by the vessel, where the trajectory follows a curved path before aligning with the reference model's straight line. This indicates that the reference model guides the vessel smoothly towards the setpoint, and the DP system effectively controls the vessel's velocity to match the reference trajectory. The overall performance shows that the system accurately tracks the reference velocity trajectories, minimizing deviations and oscillations.

7.5 Simulation 4

Scenario

The final simulation involves a DP 4 corner test, where the vessel moves through a series of setpoints in a defined sequence: - $\eta_0 = [0, 0, 0]$ - $\eta_1 = [50, 0, 0]$ - $\eta_2 = [50, -50, 0]$ - $\eta_3 = \left[50, -50, -\frac{\pi}{4}\right]$ - $\eta_4 = \left[0, -50, -\frac{\pi}{4}\right]$ - $\eta_5 = [0, 0, 0]$

The vessel must stabilize at each setpoint before proceeding to the next. The position and heading are plotted until steady state is achieved, with the desired trajectory shown for comparison. If the reference model includes velocity trajectories, these are also plotted.

7.5.1 4 Corner Test Results

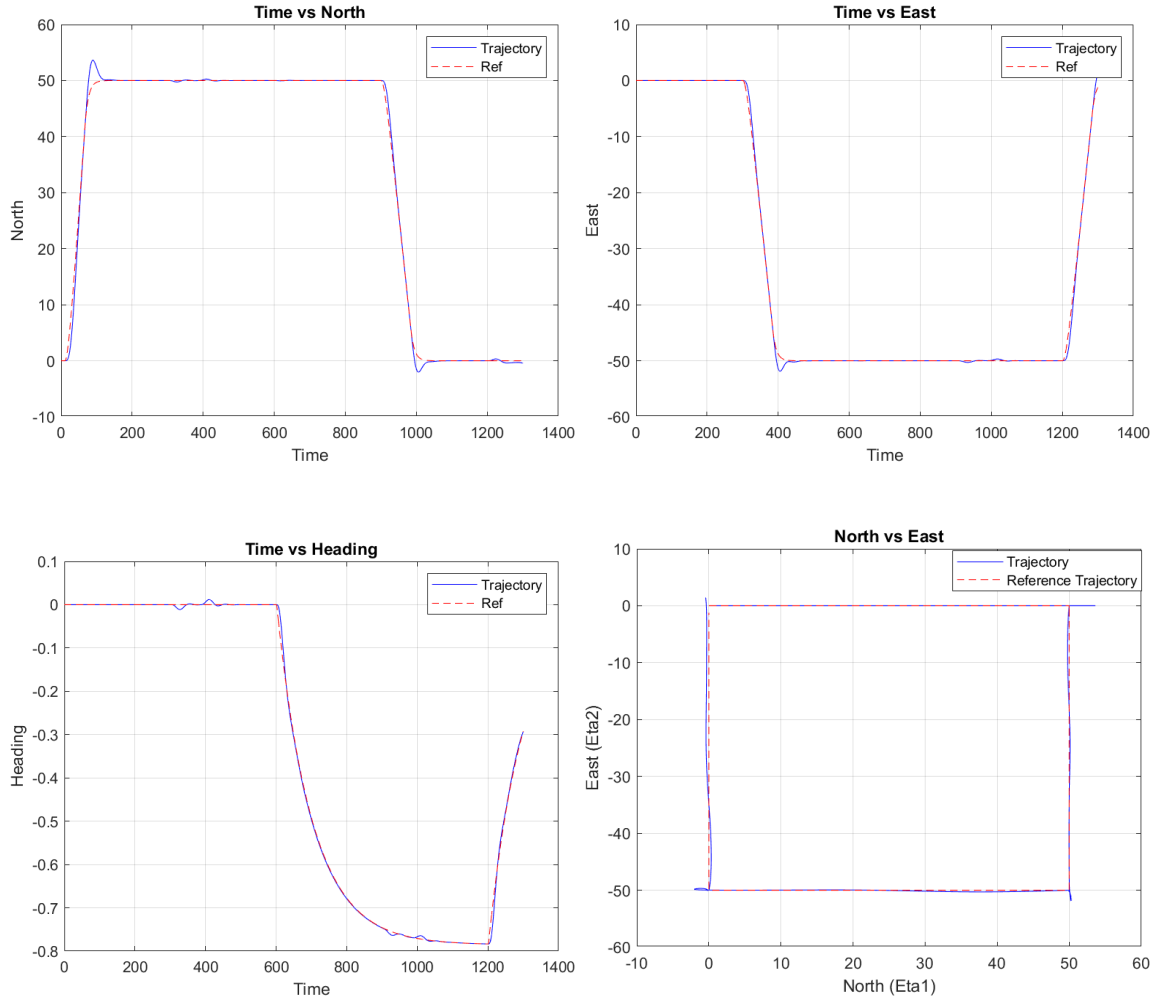

Figure 20: Simulation 4 Results

7.5.2 Discussion

In Simulation 4, the vessel performs a 4-corner test, moving through a sequence of setpoints as outlined in the scenario. The Time vs North and Time vs East plots demonstrate the vessel's movement across the specified waypoints. The vessel initially moves northward to $\eta_1 = [50, 0, 0]$, followed by a sharp eastward movement to $\eta_2 = [50, -50, 0]$. The position plots show that the vessel stabilizes at each setpoint before moving to the next. There is some initial oscillation as the vessel adjusts to the northward motion, but the overall performance is well-aligned with the reference trajectory, indicating that the Dynamic Positioning (DP) system successfully navigates through the setpoints.

The Time vs Heading plot shows the vessel's heading remaining relatively stable during the north and eastward movements until it reaches $\eta_3 = [50, -50, -\frac{\pi}{4}]$, where the heading begins to change. The heading stabilizes at $-\frac{\pi}{4}$ before moving to the final setpoint, $\eta_5 = [0, 0, 0]$. The North vs East plot illustrates the complete trajectory, with the vessel forming a square path as it moves through the setpoints. The vessel accurately follows the reference trajectory, demonstrating the DP system's ability to manage sharp turns and hold steady at each setpoint before proceeding.

7.5.3 Reference Model Velocity Trajectories

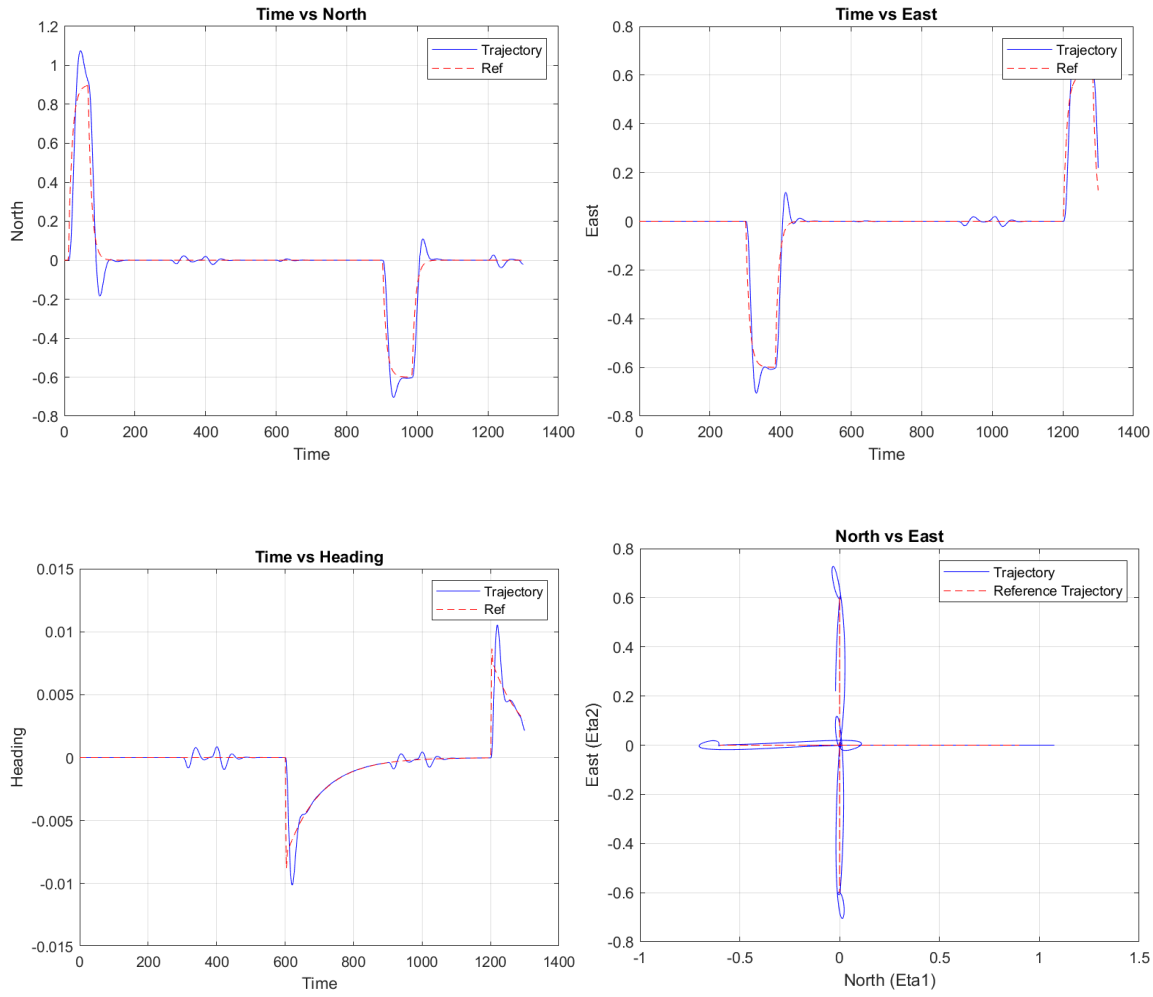

Figure 21: 4 Coner Test Velocity Trajectories

7.5.4 Discussion

The velocity trajectories for the 4-corner test, shown in Figure 20, depict the vessel's response as it moves through the sequence of setpoints. The Time vs North, Time vs East, and Time vs Heading plots reveal that the velocity initially spikes as the vessel transitions between the setpoints, particularly during the sharp turns at $\eta_2 = [50, -50, 0]$ and $\eta_4 = [0, -50, -\frac{\pi}{4}]$. These transitions introduce noticeable oscillations in both the North and East velocities, but the system quickly dampens them as the vessel stabilizes at each setpoint. The North vs East plot shows the vessel's velocity trajectory, where the sharp changes in direction during the transitions between setpoints cause the velocity to deviate from the reference trajectory. However, the vessel's velocity aligns with the reference trajectory after each setpoint is reached, indicating that the DP system effectively controls the vessel's velocity despite the challenging maneuvers in the 4-corner test.

References

[1] Asgeir J. Sørensen. *Marine Cybernetics: Towards Autonomous Marine Operations and Systems.* Lecture Notes for TMR4240 and TMR4515 Marine Control Systems, Norwegian University of Science and Technology, Trondheim, Norway, 2018.

[2] Thor I. Fossen. *Handbook of Marine Craft Hydrodynamics and Motion Control.* John Wiley & Sons Ltd, First Edition, 2011. ISBN: 978-1-119-99149-6.